A genetic algorithm-based procedure for 3D source identification at the Borden emplacement site

Xin Jin, G. (Kumar) Mahinthakumar, Emily M. Zechman and Ranji S. Ranjithan

ABSTRACT

Finding the location and concentration of groundwater contaminant sources typically requires the solution of an inverse problem. A parallel hybrid optimization framework that uses genetic algorithms (GA) coupled with local search approaches (GA-LS) has been developed previously to solve groundwater inverse problems. In this study, the identification of an emplaced source at the Borden site is carried out as a test problem using this optimization framework by using a Real Genetic Algorithm (RGA) as the GA approach and a Nelder–Mead simplex as the LS approach. The RGA results showed that the minimum objective function did not always correspond to the minimum solution error, indicating a possible non-uniqueness issue. To address this problem, a procedure to identify maximally different starting points for LS is introduced. When measurement or model errors are non-existent or minimal it is shown that one of these starting points leads to the true solution. When these errors are significant, this procedure leads to multiple possible solutions that could be used as a basis for further investigation. Metrics of mean and standard deviation of objective function values was adopted to evaluate the possible solutions. A new selection criterion based on these metrics is suggested to find the best alternative. This suggests that this alternative generation procedure could be used to address the non-uniqueness of similar inverse problems. A potential limitation of this approach is the application to a wide class of problems, as verification has not been performed with a large number of test cases or other inverse problems. This remains a topic for future work.

Key words | environmental forensics, evolutionary computation, groundwater source identification, inverse problems

Xin Jin
G. (Kumar) Mahinthakumar (corresponding author)
Ranji S. Ranjithan
Department of Civil, Construction and Environmental Engineering,
North Carolina State University, NC 27695,
USA
Tel.: +1 919 515 7696
E-mail: *gmkumar@ncsu.edu*

Emily M. Zechman
Department of Civil Engineering,
Texas A&M University, TX 77843,
USA

INTRODUCTION

Finding the location and concentration of contaminant sources is an important step in groundwater remediation and management. This could be used in identifying the responsible parties in a groundwater contamination incident and for other environmental forensic investigations. This typically requires the solution of an inverse problem from a set of measured data. The commonly used method is simulation–optimization. The solution to the inverse problem, which is frequently investigated in the field of groundwater science and engineering, involves the adjustment of model parameters of a simulation model to fit the output of the model to the observed data (Sun 1994).

Mahar & Datta (1997) developed a methodology to combine the groundwater pollutant source identification and the optimal monitoring network design. They used least-squares minimization for the source identification model and integer programming for the monitoring design model. A limitation of this work is that uncertainty

doi: 10.2166/hydro.2009.002

was not sufficiently included in the aquifer parameters. Mahar & Datta (2001) extended the work to include both hydraulic conductivity and source location in their optimization model.

Sciortino *et al.* (2000) studied the inverse modeling for locating the DNAPL in groundwater flow. Their algorithm is valid for a dissolving one-component DNAPL pool situated at the bottom of a three-dimensional homogeneous aquifer under steady, unidirectional flow conditions. The problem is formulated as a least-squares minimization problem, which they solved using the Levenberg–Marquardt algorithm. They found that the proposed inverse modeling is robust in the presence of measurement errors, but is still sensitive to the observation well location and that the solutions are non-unique.

Mahinthakumar & Sayeed (2005) proposed a hybrid genetic algorithm–local search approach (GA-LS) to solve the groundwater source identification problem. Numerical experiments showed hybrid methods to be promising because they combine the good aspects (e.g. ability to combine aspects of the solution from different parts of the decision space) of global search methods (e.g. genetic algorithms) and local search methods (gradient or non-gradient). This work, and related work by Sayeed (2004) and Clayton (2005), suggested that source identification problems are prone to non-uniqueness, especially if the location, size and strength of the source are all unknown. Hybrid methods were then extended to solve groundwater source release history problems by Mahinthakumar & Sayeed (2006). They found that hybrid methods are effective in solving these problems and that release history problems were less prone to non-uniqueness compared to source identification problems.

Non-uniqueness in solutions to inverse problems is an issue that must be addressed and is a major focus of this work. Generation of alternative solutions (i.e. identifying niches in solution space) offers a viable approach for addressing the non-uniqueness issue. In this study, the alternative generation method EAGA (Evolutionary Algorithm to Generate Alternatives (Zechman & Ranjithan 2004, 2007)) is explored as a means to address the non-uniqueness issue in inverse problems.

The goal of this study is to investigate the application of EAGA in conjunction with the GA-LS method to address the non-uniqueness issue when solving an inverse problem. In this study, a three-dimensional field scale identification of the emplaced source at the Borden site, Ontario, Canada was solved to test this optimization framework. The next section introduces the Borden site problem briefly, and discusses the governing equation and the methods used in this study. The third section presents the results and discussion. The fourth section discusses the application of the alternative generation method. The last section summarizes the major conclusions.

BORDEN SITE PROBLEM DESCRIPTION

The Borden site is a field experiment research site at a Canadian Force Base (CFB). A large number of field experiments (e.g. Mackay *et al.* 1986, 1994; Poulsen & Kueper 1992; Kueper *et al.* 1993; Rivett *et al.* 2001) were done at that site. A controlled field experiment to study the development of dissolved chlorinated solvent plumes from a residual DNAPL (dense non-aqueous phase liquid) was conducted by Rivett *et al.* (2001). Figure 1 shows a sketch of the experiment. This experiment used an emplaced source with three pollutant components, i.e. trichloromethane (TCM), trichloroethene (TCE) and perchloroethene (PCE). Measurements were made of the pollutant concentration at several downstream locations to monitor the fate and transport under natural aquifer conditions. The plumes for the three substances are found to be narrow in the transverse direction and long in the longitudinal direction due to the low transverse dispersivity.

In this study, the parameters from the Borden site field experiment were used to generate measurement data for an

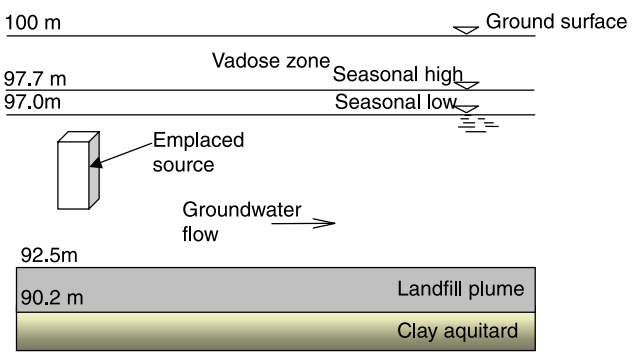

Figure 1 | Sketch of tracer test at Borden Site, Ontario, Canada.

inverse problem where the source is to be identified based on the data. The governing equation describing the groundwater transport is (Bear 1972)

$$\frac{\partial C}{\partial t} = \nabla\cdot(D\nabla C) - \nabla\cdot(Cv) + \frac{q}{\theta}(C_0 - C) \quad (1)$$

where C is contaminant concentration, D is the dispersivity tensor that is dependent on velocity, v is the velocity field, q is the flux of source or sink, C_0 is the injected source concentration and θ is porosity.

A forward simulation model based on Equation (1) and called PGREM3D (Parallel Groundwater Transport and Remediation Codes) (Mahinthakumar 1999) was used to predict downstream plume concentration for the Borden site test problem. The model was first calibrated by selecting an appropriate realization of the heterogeneous hydraulic conductivity field that leads to a modeled contaminant plume that closely matches published field measurements reported by Rivett *et al.* (2001). The randomly heterogeneous hydraulic conductivity field was generated by a turning bands algorithm (Tompson *et al.* 1989) using previously published statistical parameters for the Borden site (Sudicky 1986). This method is an unconditional method, i.e. the field of hydraulic conductivity only matches the statistical parameters of the study area. Table 1 lists the statistical parameters of hydraulic conductivity for the Borden site. Figure 2 shows the hydraulic conductivity field for a typical horizontal layer. The simulated and measured plumes are shown in Figure 3.

INVERSE MODELING METHODOLOGY

The emplaced source location and concentration are determined based on the generated measurement data

Table 1 | Statistical parameters of hydraulic conductivity for Borden site

Parameters	Value
Mean (m/d)	5.478
Standard deviation (m/d)	0.7
Correlation scale x_1 (m)	2.8
Correlation scale x_2 (m)	2.8
Correlation scale x_3 (m)	0.12

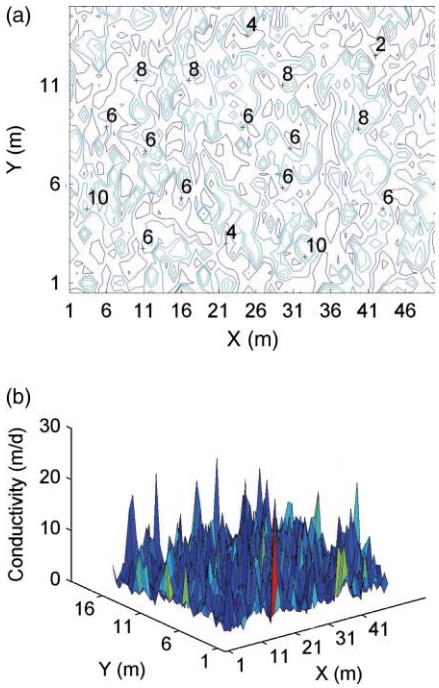

Figure 2 | Contour (a) and surface (b) plot for hydraulic conductivity field in a typical horizontal layer at the Borden site.

using the forward simulation model. The commonly used objective function for source identification is root square error (RSE, Mahinthakumar & Sayeed 2005) or normalized weighted RSE (Mahar & Datta 1997). But intial experimentation on the comparison of the two-norm and infinity-norm indicated that using the infinity-norm or

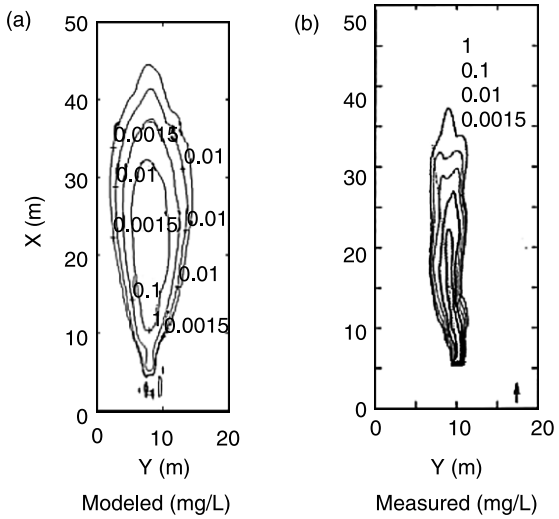

Figure 3 | Modeled (a) and measured (b) plume (TCM) at the site.

'maximum observation error' yielded slightly better results (Zechman 2005). Thus, in this study, the objective function ('objective error') to be minimized is defined as

$$\text{maximum observation error} = \max_{k\in \text{nt},\, \text{iob}\in \text{nob}} \left\{ \left(ccal_{\text{iob}}^{k} - cobs_{\text{iob}}^{k} \right)^2 \right\} \quad (2)$$

where $ccal_{\text{iob}}^{k}$ and $\text{cobs}_{\text{iob}}^{k}$ are the calculated and observed contaminant concentrations, respectively, at time k and observation location iob; nt is the total number of time steps; nob is the total number of observation wells. One might argue that the objective function represented by Equation (2) favors only the larger concentration differences to be minimized. While this is true to an extent, it is also true that larger concentrations indicate a stronger signal from the source and these are more important than the smaller values. Moreover, as the iteration progresses the larger differences are progressively minimized and the smaller differences gradually become more important.

To solve the inverse problem, this study used a simulation–optimization approach based on a parallel hybrid GA-LS approach that couples a real-valued genetic algorithm (RGA) search with a Nelder–Mead simplex (NMS) search. This hybrid approach is henceforth referred to as RGA + NMS. Simulation–optimization approaches are widely used in groundwater remediation system design and management. It combines the groundwater forward simulation with mathematical optimization. This approach is based on an iterative process that requires many forward model evaluations and computationally more intensive than the corresponding forward model. As the forward model computations are independent in a generation of RGA parallel processing was used to facilitate the computation. Parallel computation implementation details are available in Sayeed & Mahinthakumar (2005). In this study, 57 processors of the NCSA TeraGrid Cluster[1] were used to do the independent forward simulations modeling in parallel. A complete simulation–optimization model takes about 20 minutes. As the actual location and concentration of the source are also known in this case, the performance with respect to the accuracy of the solutions predicted by each approach is also evaluated.

The monitoring network layout is selected downstream. They are at elevations of 2, 3 and 5 m above the bottom of the study area. Figure 4 shows the layout and lists the coordinates of the sampling points.

In the representation of the source identification problem, the source was assumed to be a rectangular prism with uniform concentration within this prism. This leads to seven unknowns (i.e. decision variables): three coordinates (x, y, z) each to denote the two extremities of the prism, and a concentration. Since the real location and concentration of the source is known for this illustration study, we can define the following metric as a measure of

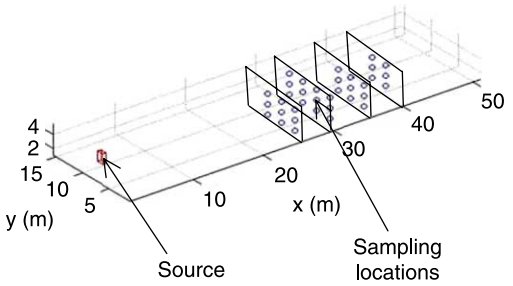

No.	Sampling points	No.	Sampling points	No.	Sampling points
1	(26,3,2)	13	(26,3,3)	25	(26,3,5)
2	(26,6,2)	14	(26,6,3)	26	(26,6,5)
3	(26,8,2)	15	(26,8,3)	27	(26,8,5)
4	(31,3,2)	16	(31,3,3)	28	(31,3,5)
5	(31,6,2)	17	(31,6,3)	29	(31,6,5)
6	(31,8,2)	18	(31,8,3)	30	(31,8,5)
7	(31,11,2)	19	(31,11,3)	31	(31,11,5)
8	(36,3,2)	20	(36,3,3)	32	(36,3,5)
9	(36,6,2)	21	(36,6,3)	33	(36,6,5)
10	(36,8,2)	22	(36,8,3)	34	(36,8,5)
11	(41,6,2)	23	(41,6,3)	35	(41,6,5)
12	(41,8,2)	24	(41,8,3)	36	(41,8,5)

Figure 4 | Sketch and coordinates of sampling locations of monitoring well layout.

[1] http://www.ncsa.uiuc.edu/UserInfo/Resources/Hardware/TGIA64LinuxCluster/

performance of the optimization algorithms:

$$\text{solution error} = \frac{1}{\text{np}} \sum_{i=1}^{\text{np}} \frac{|p_i^{\text{calc}} - p_i^{\text{exact}}|}{p_i^{\text{exact}}} \times 100 \quad (3)$$

where p_i^{calc} and p_i^{exact} are the calculated and exact values, respectively, for variable i and np is the number of variables ($= 7$ in this illustration).

RESULTS FOR RGA + NMS

For the RGA + NMS procedure, the population size for RGA is set to 200 and the maximum number of generations is 20. Binary tournament selection is adopted. The crossover rate is 0.7 and the mutation rate is 0.05. The maximum number of iterations for NMS is also set to 20. The above values were chosen through initial experimentation using a set of values within typical ranges for each parameter. The crossover and mutation values are within typical ranges (0.5–0.8 for crossover and 0.01–0.1 for mutation) for real encoded problems (Michalewiz 1996). Real encoding is appropriate for this problem as the source is represented by seven real variables. The number of generations was cut off at 20 for RGA, as the primary purpose of RGA is to provide starting points for the local search and a slow rate of convergence was observed beyond 20 generations. A total of 10 trials with different random seeds were tested. The change of objective function values and solution error for RGA + NMS is shown in Figure 5 for a typical trial. It is evident that, while the objective function value (i.e. objective error) decreased consistently, the solution error metric does not always monotonically decrease. The real source location and the identified source location using RGA + NMS are compared in Figure 6. While the location of the centroid is approximately captured by the algorithm, the size and concentration are not. This is possibly due to several interrelated factors, such as inadequate observation data, weak signals or non-uniqueness. Lack of observation data or improper sampling of data will impact solution accuracy. In general, more observation data in the downstream region will improve the solution accuracy. Figure 7 shows the comparison of solution errors obtained by two different observation well layouts. It suggests that, as the

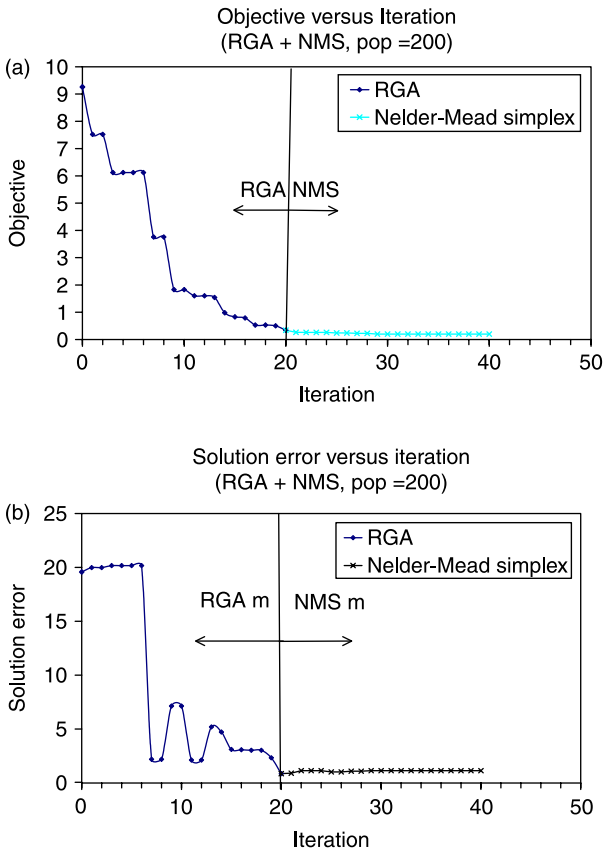

Figure 5 | Convergence behavior of RGA and NMS for (a) objective error, (b) solution error.

number of observation wells is increased, more information was incorporated, resulting in increased solution accuracy. Signatures representing size and concentration information may only be weakly embedded in the observed data as they can be easily marred by dispersion. Non-uniqueness is possible as a source with larger concentration and smaller size may lead to similar concentration observations as one

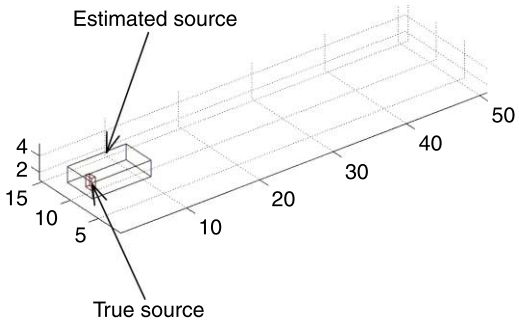

Figure 6 | Best solution using standard RGA + NMS.

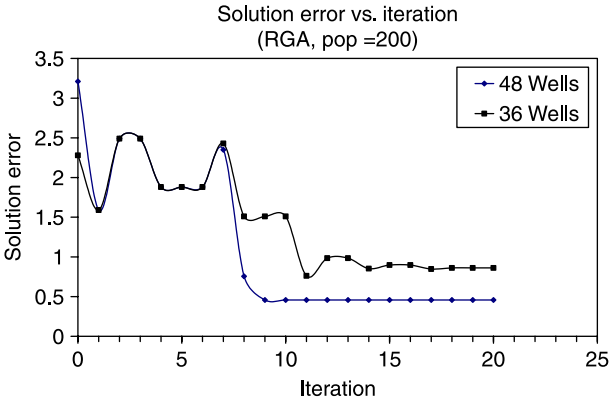

Figure 7 | RGA convergence behavior in terms of solution error for different observation well layouts.

with smaller concentration and larger size since both may have similar mass loading. The non-uniqueness issue is investigated further in subsequent sections.

If there are no measurement or model errors, it is very unlikely that there is true non-uniqueness for this problem, i.e. there is only one solution that will result in an objective function value of exactly zero. However, as indicated schematically in Figure 8, there may be several 'solutions' that may have low objective values. Four such solutions are shown in Figure 8: we term this 'pseudo' non-uniqueness or non-uniqueness above a certain threshold objective value. Given that a GA is a good global searcher but is weak at refined local search, it may identify several near-optimal solutions. A subsequent local search starting from these solutions may lead to the true solution. This problem may be exacerbated due to lack of adequate observations or noise due to measurement or other errors. Likelihood of

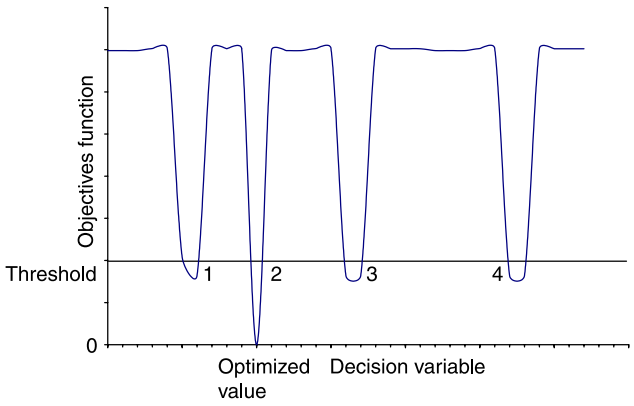

Figure 8 | Schematic illustration of non-uniqueness feature of inverse problem without any measurement error.

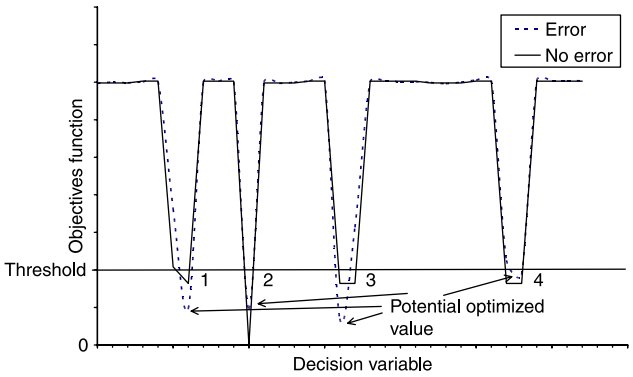

Figure 9 | Schematic illustration of non-uniqueness feature of inverse problem with measurement error (noise).

non-uniqueness will generally increase if measurement or other errors exist in the objective function, as shown schematically in Figure 9. In this case, it is very difficult to estimate the true solution as it may have erroneously a higher objective function value than other local optima. In this case, several local optima might be identified as potential solutions for the studied inverse problem.

ADDRESSING NON-UNIQUENESS

To address non-uniqueness we propose using a technique called alternative generation (AG). AG can provide multiple maximally different solutions in decision space that have similar objective values. These solutions could then be used as starting points for a local search approach. As depicted in Figure 8, if AG is utilized, it may find all four alternative threshold solutions from which four local searches could be started. In this case, the local search starting from alternative 2 will lead to the true solution. Recently, various AG approaches have been developed for evolutionary methods using niching techniques. In this paper, we adopt the EAGA approach proposed by Zechman & Ranjithan (2004, 2007) and modified slightly by Sayeed (2004). The following is a brief description of this algorithm:

Step 1: initialize the population with P subpopulations (in this study, 4 subpopulations each with a size of 50 were chosen).

Step 2: In SP_1, search for the best solution with respect to the objective function.

Step 3: In the remaining subpopulation SP_p, $p = 2, 3, \ldots, P$, calculate the fitness of each individual and assign a 'feasible' flag for the solutions that are within the relaxed target and an 'infeasible' flag for the others. The relaxed target indicates how much of the fitness domain will be explored. For example, if the objective is to minimize Equation (2) and the least objective in a given iteration is O_{opt}, the target could be set as $(1 + \alpha)\, O_{opt}$, where α is a relaxation coefficient. In this study, α was linearly varied from 0.5 (generation 0) to 0.2 (generation 20) so as to shift gradually from exploration to exploitation as the iteration progressed.

Step 4: For each individual k in a subpopulation SP_p, $p = 2, 3, \ldots, P$, calculate the distance measure (d_k) between individual k and the already generated alternatives in the preceding subpopulations, i.e. $SP_1, \ldots, SP_{p-1}$ as defined by Sayeed (2004):

$$\text{distance} = \sqrt{\sum_{i=1}^{n} (x_i - y_i)^2} \tag{4}$$

where n is the number of decision variables, $x = (x_1, x_2, \ldots, x_n)$ is individual k and $\boldsymbol{y} = (y_1, y_2, \ldots, y_n)$ is the already generated alternative solutions.

Step 5: In each subpopulation SP_p, apply binary tournament selection. In SP_1, the selection is based on the objective function value. In SP_p, $p = 2, 3, \ldots, P$, the selection is based on both objective and distance values. If two individuals are feasible, the one with the larger distance value (d_k) will be selected. For the other cases, if the majority of the subpopulation is feasible, the selection is still based on distance value. Otherwise, the selection is based on objective function value.

Step 6: Apply other genetic algorithm operators, such as crossover and mutation.

Step 7: Check the stopping criteria. If it is met, stop the algorithm. Otherwise go to step 2.

The choice of the number of subpopulations in Step 1 depends on the degree of non-uniqueness of the problem. A larger number of subpopulations may be needed if the non-uniqueness is high. Unfortunately, in many situations one may not know the degree of non-uniqueness prior to solving the problem. In these cases, one might start with a few subpopulations and check if the resulting solutions are vastly different. In such a case, the number of subpopulations chosen is too small. If at least two of the solutions resulting are close in the decision space, then the number of subpopulations chosen is sufficient. We used 4 subpopulations, as this was found to be a good starting point for this problem. The size of each subpopulation was fixed at 50 to maintain the same total population size (200) of the RGA runs.

Case with no measurement error

The EAGA described above was used to generate four alternative solutions. A total of 10 trials, each with a different initial population, were tested. For the first alternative, these trials exhibited a coefficient of variation of 0.277 for the objective error, indicating the variation among trials is acceptable. Additional details regarding these trials including figures showing the error bars are available in the PhD dissertation of Jin (2008). Figure 10 compares the objective and solution errors for each of these alternatives for a typical trial. It is interesting to note that, while a4 has the biggest objective error, it also has the smallest solution error. In contrast, a1 and a2 have the smallest objective errors and the biggest solution errors. While this illustrates an extreme case, this shows that any one of the 4 alternatives could lead to the true solution. In a typical real situation where the solution error cannot be calculated, one could further examine all 4 solutions either by conducting additional field investigations or by

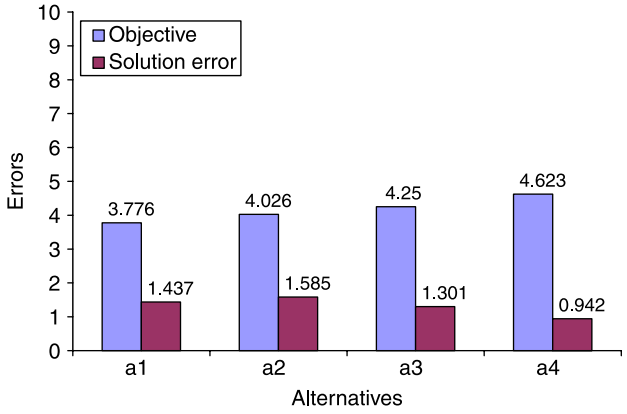

Figure 10 | Comparison of objective and solution errors for four different alternatives before local search (RGA + EAGA).

incorporating new information. In our case, however, we will use these solutions as starting points for a local search. The solutions yielded by these extreme cases (a2 and a4) are compared in Figure 11.

We next apply four instances of a local search algorithm (Nelder–Mead simplex) by using these four alternatives as starting points. Figure 12 compares the objective versus solution error for each alternative. As expected, a4 leads to the best solution since it starts with a smaller solution error. Figure 13 compares the predicted and true solutions for the best (a4) and worst (a2) cases. It is interesting to note that the resulting solutions from the local searches do not have the previous anomaly between the objective and solution errors. This suggests that below a threshold the objective value correlates well with the solution error for all four alternatives, indicating that non-uniqueness is not an issue if we can sufficiently reduce the objective error. This implies that, after RGA + EAGA + NMS, we can select the solution with the minimum objective value as the final solution since it likely corresponds to the smallest solution error. But this statement may not hold true for cases using observation data with measurement errors, as the threshold will likely rise with increasing errors. This case is studied next.

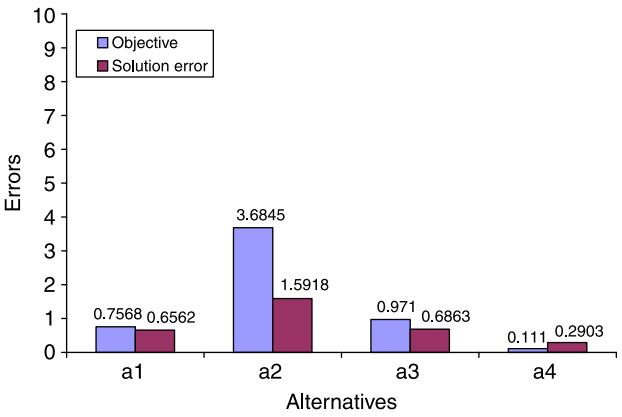

Figure 12 | Comparison of objective and solution errors for four different alternatives after local search (RGA + EAGA + NMS).

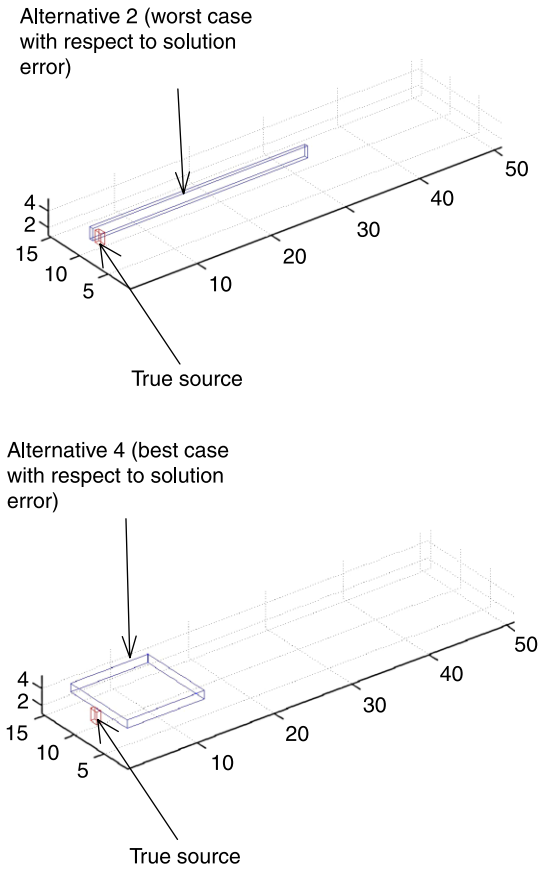

Figure 11 | Best and worst alternative solutions for the Borden site problem with only RGA + EAGA.

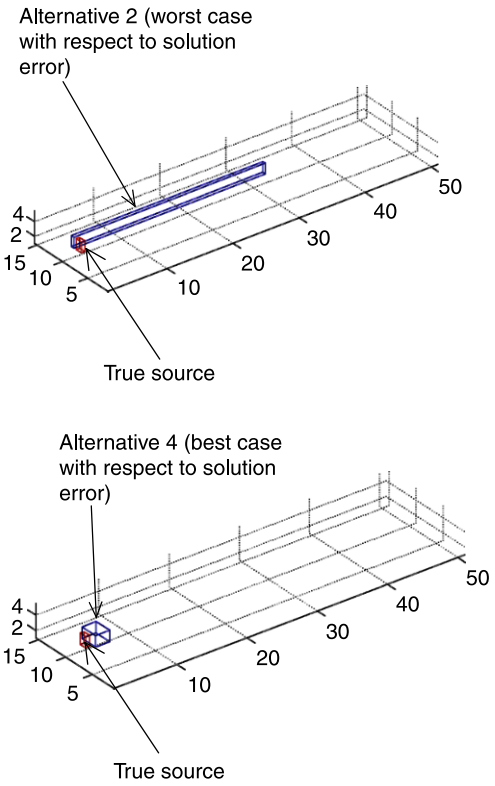

Figure 13 | Best and worst alternative solutions for the Borden site problem after local search.

Case with non-zero measurement error

In this case, additional numerical tests were conducted by introducing artificial errors in the synthetic measurement data. In this test a uniformly distributed random white noise was added to the synthetically generated concentration observations to simulate measurement error:

$$C_{\text{iob}}^{\text{obs}} = [1 + nl(r - 0.5)]C_{\text{iob}}^{\text{gen}} \quad (5)$$

where $C_{\text{iob}}^{\text{obs}}$ is observed concentration and $C_{\text{iob}}^{\text{gen}}$ is synthetically generated concentration at the observation location iob, nl is the noise level (e.g. for 10%, it is 0.1) and r is a uniform random number between 0 and 1. It is noted that normally distributed noise ($n[0,1]$) is sometimes used to represent measurement error (Mahar & Datta 1997). A uniform distribution is generally more conservative as its values are not concentrated around 0 as in a normal distribution.

Figures 14 and 15 show the minimized 'max observation error' versus solution error before and after local search for 1% white noise. These figures show that the basic aspects of the previous results still hold, with the exception of some minor variations in the specific values. Again, after local search, the minimum objective error corresponds to the minimum solution error. However, this time alternative 3 led to a better solution than alternative 4.

Figures 16 and 17 shows the results for 10% white noise. As expected, both the objective function and solution error are higher than those corresponding to the 1% white noise case depicted by Figures 14 and 15, respectively. Also, the smaller objective function does not now correspond to the smaller solution error. This implies that, with increased measurement errors, the RGA + EAGA + NMS method may identify at best potential non-unique solutions but not pinpoint the correct solution. Since the objective function value is no longer a good indicator, it is desirable to define new metrics to characterize the accuracy of the alternative solutions. The basis for these metrics is built upon a measure of sensitivity of the predicted concentrations at the observation locations due to changes in the source characteristics of a solution. For example, incremental changes in the source location and concentration would result in changes in the observation error. An aggregate measure of the changes resulting from multiple realizations

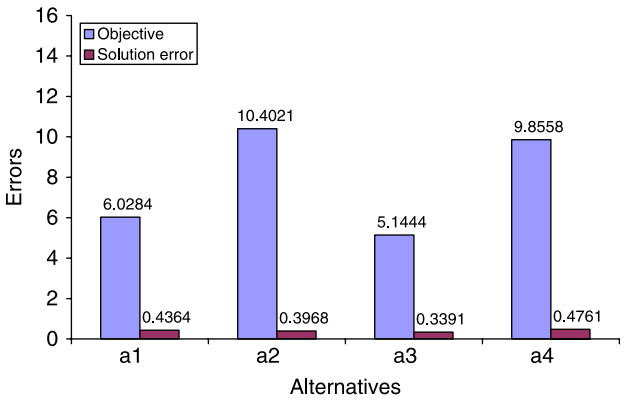

Figure 15 | Comparison of objective and solution errors for different alternatives after local search with 1% measurement error (RGA + EAGA + NMS).

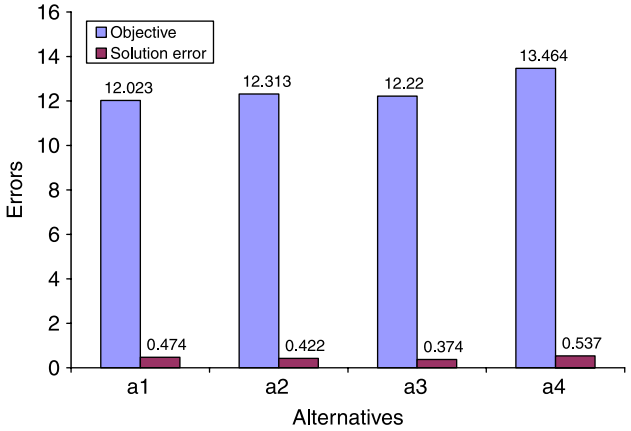

Figure 14 | Comparison of objective and solution errors for different alternatives with 1% measurement error (RGA + EAGA) before local search.

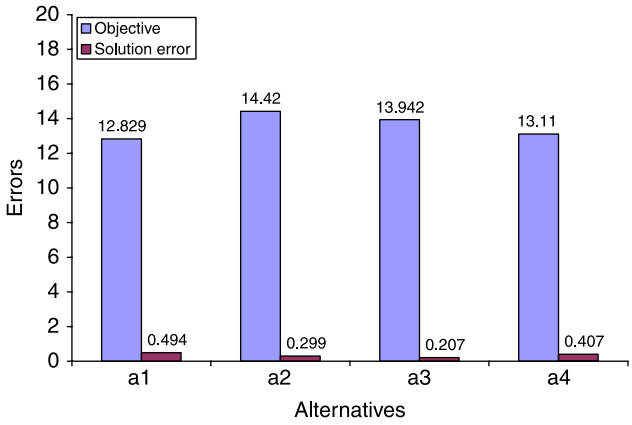

Figure 16 | Comparison of objective and solution errors for four different alternatives before local search with 10% measurement error (RGA + EAGA).

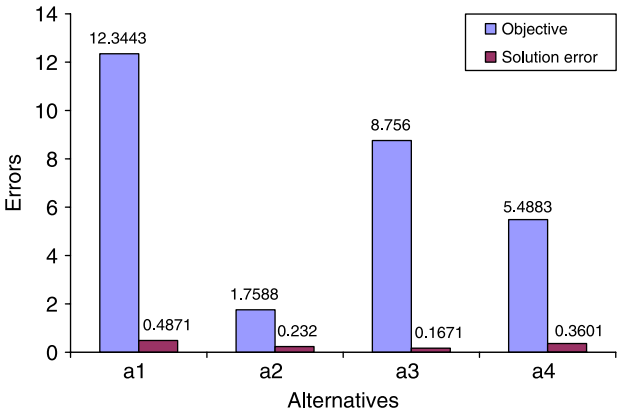

Figure 17 | Comparison of objective and solution errors for four different alternatives after local search with 10% measurement error (RGA + EAGA + NMS).

of random perturbations of the source characteristics is used in this investigation. We define two metrics that relate to the objective function as follows:

$$\text{MO} = \text{mean of objective function values} = \frac{1}{N}\sum_{i=1}^{N}(\text{maximum observation error})_i \quad (6)$$

$$\text{STDOBJ} = \text{stardard deviation of objective function values} = \text{std}\{(\text{maximum observation error})_i\}$$

where N is the total number (e.g. 1,000) of realizations. Low values are desirable for both MO and STDOBJ. A lower MO indicates that this alternative performs reasonably well in the presence of noise in terms of the objective function value. A lower STDOBJ indicates that this alternative is robust in the presence of noise (i.e. less sensitive to noise). The error considered in Equation (5) is 'unbiased' (a mean of zero) which is generally appropriate for measurement errors. Thus MO and STDOBJ could be used as the metrics for evaluating the four alternatives. It is noted that if other sources of errors such as model structure error (e.g. error in hydraulic conductivity distribution) need to be considered then errors could be biased and these metrics may not be good indicators.

Table 2 lists the MO and STDOBJ values for four alternatives generated using 1,000 realizations of measurement error for 30 cases, each with a different initial random seed for the RGA (i.e. each case with a different initial population). For illustrative purposes these values are depicted in Figure 18 for case 5. From Figure 18 and Table 2, comparing a1–a4, it is shown that, for each case, the four alternatives have very different performances in terms of MO or STDOBJ. Which alternative is to be selected depends on the metric of interest and metric values for each alternative. For example, for case 1, in terms of MO, the best alternative is a4, while in terms of STDOBJ, the best alternative is a1. Several other cases (e.g. cases 6 and 10) also show similar behavior. But for the remaining cases, the best alternatives in terms of both metrics are the same.

The solution error values are also listed in Table 2. It shows that the best alternative might be other than those deemed good in terms of MO or STDOBJ. For example, for case 10, in terms of solution error, the best alternative is a2. But in terms of MO and STDOBJ, the best alternatives are a3 and a1, respectively.

From the above analysis, it is shown that different metrics will result in different best alternatives. How to choose the best one when multiple alternatives are available is still an open question. This question could be addressed by using both the MO and STDOBJ metrics in the selection process (method 1) in the following manner (Figure 19 shows the flowchart for this procedure):

1. Choose the two best alternatives in terms of MO and STDOBJ, respectively. The two alternatives might be different.

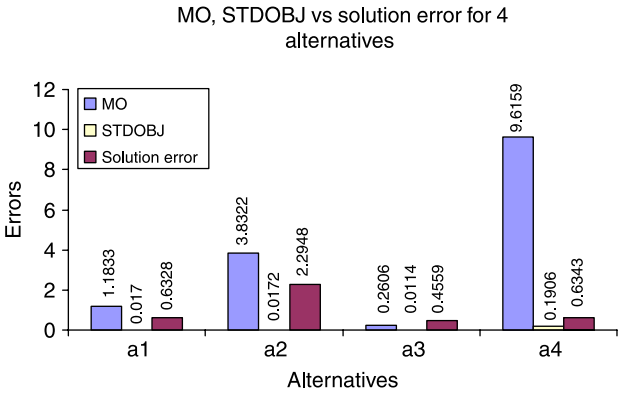

Figure 18 | Comparison of mean objective and standard deviation (1,000 realizations) of different alternatives after local search with 10% measurement error (RGA + EAGA + NMS).

Table 2 | Mean of objective function values (MO) and standard deviation of objective function values (STDOBJ) of 1000 realizations of observations for 4 alternatives after local search with 10% noise error for 30 cases (bold or underlined numbers are selected alternatives: bold represents the cases that the selected alternative is the best one in term of solution error; underline represents the opposite)

	Alternative 1				Alternative 2				Alternative 3				Alternative 4			
Case	Objective	MO	STDOBJ	Solution	Objective	MO	STDOBJ	Solution	Objective	MO	STDOBJ	Solution	Objective	MO	STDOBJ	Solution
1	2.4807	2.4796	0.0118	0.8149	1.4663	1.4833	0.0387	0.7403	1.653	1.6272	0.0192	0.6231	0.9302	**0.9286**	0.0121	0.5523
2	0.8433	0.9156	0.0675	0.5648	0.8486	0.8951	0.0496	0.5954	0.964	1.0836	0.0685	0.5673	0.314	**0.3492**	**0.0281**	0.5269
3	9.4721	9.5926	0.181	0.4857	0.9349	1.0368	0.0768	0.6672	0.2182	**0.232**	**0.0192**	0.3999	9.6193	9.7433	0.1905	0.4995
4	1.4296	1.4994	0.0711	0.7643	2.0653	2.1237	0.0781	0.856	9.6751	9.8162	0.1408	1.2527	2.215	2.2932	0.0737	0.6888
5	1.1697	1.1833	0.017	0.6328	3.8271	3.8322	0.0172	2.2948	0.2583	**0.2606**	**0.0114**	0.4559	9.5021	9.6159	0.1906	0.6343
6	0.076	0.094	0.0131	0.2514	9.6936	9.8143	0.115	2.0438	0.1041	0.1106	**0.0057**	0.2499	0.7662	0.8593	0.0698	0.6396
7	0.5216	**0.6394**	**0.068**	0.6139	2.921	3.1977	0.1584	0.8841	3.5434	3.8364	0.182	0.9612	9.7381	9.8655	0.1754	2.1213
8	2.7737	2.9643	0.1338	0.7953	0.1336	**0.141**	**0.0057**	0.3223	3.6676	3.7518	0.0998	2.4939	2.4081	2.4768	0.0832	0.7505
9	9.6365	9.7495	0.193	0.48	0.4614	0.5678	0.0609	0.5515	9.0709	9.1839	0.1097	2.3121	9.773	9.8919	0.1176	1.7976
10	2.0538	2.0947	0.0641	0.7883	9.608	9.728	0.1907	0.4248	1.4163	1.4662	0.0675	0.6662	3.7122	3.7684	0.0795	2.141
11	1.5076	1.5721	0.0977	0.6868	3.0893	3.1976	0.1323	0.8676	9.8372	9.9074	0.1023	0.8935	1.4172	**1.5001**	**0.0862**	0.5891
12	0.665	0.6885	0.0278	0.6087	0.4967	0.5455	0.0433	0.5776	0.8574	0.8793	**0.0237**	0.5474	9.921	9.9499	0.1452	3.9745
13	0.2707	0.297	**0.0281**	0.3847	1.8724	1.9299	0.1094	0.7008	0.207	0.2185	0.0462	0.446	1.8451	1.9139	0.1109	0.8108
14	1.3581	1.3971	0.0522	0.3888	3.7593	3.7853	0.0513	2.4122	0.3882	0.3923	0.0145	0.4963	0.142	**0.1535**	0.025	0.3503
15	0.3769	**0.3833**	**0.0129**	0.4844	0.7553	0.7486	0.0158	0.5428	2.9307	3.0451	0.1145	0.9504	0.5754	0.5906	0.0162	0.5548
16	0.412	**0.4264**	**0.0267**	0.5266	0.8031	0.8585	0.0632	0.6761	2.3166	2.4148	0.1088	0.8003	2.1881	2.2841	0.0982	0.8274
17	9.921	9.9161	0.1919	2.1264	1.196	**1.2624**	**0.0951**	0.5273	3.7984	3.9102	0.1787	2.652	4.0162	4.1172	0.1882	1.3329
18	2.9695	3.0955	0.1262	0.6259	1.4513	1.5124	0.0725	0.5973	8.9996	9.0306	0.1856	0.4524	9.1357	9.2254	0.097	2.0848
19	0.0919	**0.1059**	**0.0161**	0.3416	0.6302	0.6345	0.0624	0.4322	0.3864	0.3915	0.0458	0.4718	3.8013	3.8123	0.0294	1.9862
20	1.793	1.8742	0.1035	0.6654	0.4218	0.4644	0.0408	0.4572	1.1194	1.1832	0.0789	0.5354	0.1581	**0.1883**	**0.0265**	0.4452
21	2.5702	2.7159	0.1608	0.6829	3.5437	3.7783	0.1575	1.7504	0.7747	0.8714	0.0778	0.6079	0.5213	**0.5388**	**0.0133**	0.2552
22	0.9445	0.8902	0.0539	0.6159	3.1559	3.1618	0.0036	0.8466	10.0565	10.0524	0.0161	0.9939	0.1306	**0.1214**	0.0117	0.3623
23	6.75	7.0148	0.2058	1.2892	9.8682	9.9282	0.1883	5.4061	3.7045	3.7623	0.08	2.3593	9.8682	9.9307	0.1889	5.4591
24	0.291	0.259	0.0309	0.4671	0.1214	**0.1481**	**0.0231**	0.2706	1.6458	1.6325	0.0821	0.6735	3.2641	3.471	0.1702	0.8793
25	3.696	3.7547	0.083	2.4248	9.5917	9.6428	0.1954	0.4645	0.2077	**0.2211**	**0.0173**	0.4563	1.693	1.7034	0.0519	0.7653
26	1.9493	1.9728	0.1111	0.6533	1.4691	1.4579	0.0178	0.5429	2.6763	2.8349	0.1285	0.8745	0.1239	**0.1288**	**0.0084**	0.2912
27	0.4193	0.4333	0.0191	0.5346	0.3036	0.2803	0.0268	0.2587	1.7493	1.7771	0.0579	0.6388	0.2407	0.247	0.0107	0.368
28	0.0596	**0.0593**	0.0062	0.2277	3.1357	3.1554	0.0349	0.8398	0.6876	0.6801	0.0052	0.5702	0.1117	0.1196	0.006	0.3087
29	2.6266	2.7191	0.0999	0.8485	2.6375	2.6765	0.0572	0.7564	2.2158	2.3718	0.1454	0.9173	0.5212	**0.5496**	**0.0365**	0.5873
30	1.8203	1.9737	0.1235	0.8351	0.9074	1.0072	0.0737	0.5953	0.3847	**0.459**	**0.0504**	0.5711	0.7449	0.8442	0.0814	0.6194

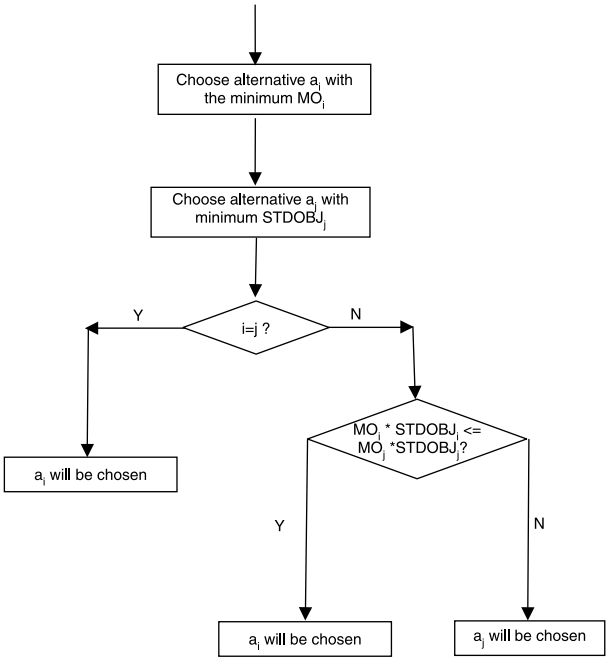

Figure 19 | Basic selection procedure (method 1) for alternatives with measurement error.

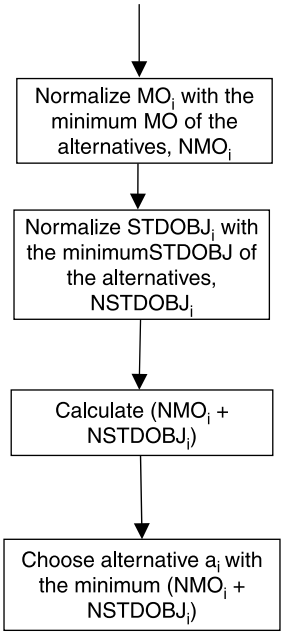

Figure 20 | Alternative selection procedure (method 2) for alternatives with measurement error.

2. If the two best alternatives from step 1 are the same, this solution will be selected as the final solution.
3. If they are different, compare their MO and STDOBJ values and calculate the relative difference, i.e. the ratio of the values between two alternatives, for each. The choice will be based on which metric has the bigger difference, MO or STDOBJ. For example, in Table 2, for case 6, in terms of MO the best alternative is a1 with a value of 0.094, while for STDOBJ the best alternative is a3 with value of 0.0057. To choose the best one, we can make the following comparison. For a1, the MO and STDOBJ are 0.094 and 0.0131, respectively, while for a3, the MO and STDOBJ are 0.1106 and 0.0057 respectively. The relative difference of MO between a1 and a3 (0.1106/0.094 = 1.18) is smaller than that of STDOBJ (0.0131/0.0057 = 2.30). Thus we make our decision based on STDOBJ and choose a3 whose STDOBJ value (0.0057) is smaller than that of a1. The above procedure is equivalent to choosing the smaller of the product of MO and STDOBJ (Figure 19).

If we apply the above criterion to the 30 cases listed in Table 2, for 24 cases out of 30, (i.e. 80% reliability), the selected alternatives also has the best solution error.

A comparison was made with another selection strategy (method 2, see flowchart in Figure 20) as described below:

1. Normalize MO and STDOBJ in terms of the lowest value in each category.
2. Sum the MO and STDOBJ values for each alternative.
3. Select the alternative with lowest summed value of MO and STDOBJ.

This method is similar to method 1. But it might find a solution whose values of either MO or STDOBJ are not the smallest, but their sum is the smallest. When applying method 2 to the same 30 cases in method 1, the selected alternatives also had the best solution error for 23 cases out of 30.

From the above analysis, it is evident that methods 1 and 2 perform nearly equally well, with method 1 yielding slightly better results. We therefore recommend that a selection strategy based on MO and STDOBJ (e.g. method 1) could be used to make a decision on the four alternatives generated by EAGA. It remains to be investigated, however, whether this process could be applied to other source identification problem scenarios or even other inverse problems.

CONCLUSION

From this study, we can conclude that a combination of RGA, EAGA and NMS could be used effectively to solve the contaminant source identification problem with reasonable accuracy. In particular, the use of EAGA effectively addresses the non-uniqueness problem by providing several alternative solutions that could be used as starting guesses for local search (i.e. NMS). This statement holds true for both perfect measurement data and for measurements with errors. For the case with zero or small measurement errors (e.g. 1%), the best solution (in terms of objective value) resulting from the local search is also the best in terms of solution (closest to the true solution). For the case with moderate measurement errors (e.g. 10%), a new alternative selection strategy based on the metrics of MO and STDOBJ is proposed. For 24 out of 30 trials conducted, this selection strategy enables selection of the alternative that is closest to the true solution. This indicates a potential robustness of this method as it could tolerate moderate measurement errors. It should be noted that the proposed method for cases with measurement errors, although based on sound intuitives, has not been proven theoretically nor verified with other applications. Whether it could be generalized to other inverse problems remains a topic for future work.

ACKNOWLEDGEMENTS

This work was partially supported by the National Science Foundation (NSF) under grant no. BES-0238623. Any opinions, findings and conclusions or recommendations expressed in this material are those of the author(s) and do not necessarily reflect the views of the NSF. The authors also wish to acknowledge the North Carolina State University and National Center for Supercomputing Applications for providing the supercomputer resources necessary for this work.

REFERENCES

Bear, J. 1972 *Dynamics of Fluids in Porous Media*. American Elsevier, New York.

Clayton, M. 2005 Groundwater contamination source identification using hybrid optimization methods. In: *ASCE World Water and Environmental Resources Congress 2005, Anchorage, AK, 15–19 May*. doi: 10.1061/40792(173)6.

Jin, X. 2008 *Optimization-based Methodologies for Detection and Monitoring of Groundwater Sources*. PhD dissertation, North Carolina State University, Raleigh, NC.

Kueper, B. H., Redman, D., Starr, R. C., Reitsma, S. & Mah, M. 1993 A field experiment to study the behavior of tetrachloroethylene below the water table: spatial distribution of residual and pooled DNAPL. *Ground Water* **31** (5), 756–766.

Mackay, D. M., Bianchi-Mosquera, G., Kopania, A. A. & Kianjah, H. 1994 A forced-gradient experiment on solute transport in the Borden aquifer:1. Experimental methods and moment analyses of results. *Water Resour. Res.* **30** (2), 369–383.

Machay, D. M., Freyberg, D. L., Roberts, P. V. & Cherry, J. A. 1986 A natural gradient experiment on solute transport in a sand aquifer: 1. Approach and overview of plume movement. *Water Resour. Res.* **22** (13), 2017–2029.

Mahar, P. S. & Datta, B. 1997 Optimal monitoring network and ground-water-pollution source identification. *J. Water Res. Plan. Manage. ASCE* **123** (4), 199–207.

Mahar, P. S. & Datta, B. 2001 Optimal identification of groundwater pollution sources and parameter estimation. *J. Water Res. Plan. Manage. ASCE* **127** (1), 20–29.

Mahinthakumar, G. (Kumar) 1999 *PGREM3D: Massively Parallel Codes for Groundwater Flow and Transport Online Manual*. Available at: http://www4.ncsu.edu/ ~ gmkumar/pgrem3d.pdf

Mahinthakumar, G. & Sayeed, M. 2005 Hybrid genetic algorithm–local search methods for solving groundwater source identification inverse problem. *J. Water Res. Plan. Manage. ASCE* **131** (1), 45–47.

Mahinthakumar, G. & Sayeed, M. 2006 Reconstructing groundwater source release histories using hybrid optimization approaches. *J. Environ. Forensics* **7** (1), 45–54.

Michalewicz, Z. 1996 *Genetic Algorithms + Data Structures = Evolution Programs*, 3rd edition. Springer-Verlag, New York.

Poulsen, M. M. & Kueper, B. H. 1992 A field experiment to study the behavior of tetrachloroethylene in unsaturated porous media. *Environ. Sci. Technol.* **26** (5), 889–895.

Rivett, M. O., Feenstra, S. & Cherry, J. A. 2001 A controlled field experiment on groundwater contaminant by a multicomponent DNAPL: creation of the emplaced–source and overview of dissolved plume development. *J. Contam. Hydrol.* **49**, 111–149.

Sayeed, M. 2004 An Efficient Parallel Optimization Framework for Inverse Problems. PhD dissertation, North Carolina State University, Raleigh, NC.

Sayeed, M. & Mahinthakumar, G. 2005 An efficient parallel implementation of hybrid optimization approaches for solving groundwater inverse problems. *J. Comput. Civil Eng.* **19** (4), 329–340.

Sciotino, A., Harmon, T. C. & Yeh, W. W.-G. 2000 Inverse modeling for locating dense nonaqueous pools in groundwater under steady flow conditions. *Water Resour. Res.* **36** (7), 1723–1735.

Sudicky, E. A. 1986 A natural gradient experiment on solute transport in a sand aquifer: spatial variability of hydraulic conductivity and its role in the dispersion process. *Water Resour. Res.* **22** (13), 2069–2082.

Sun, N.-Z. 1994 *Inverse Problems in Groundwater Modeling, Theory and Application of Transport in Porous Media*. Kluwer, Dordrecht.

Tompson, A. F. B., Aboudu, R. & Gelhar, L. W. 1989 Implementation of the three-dimensional turning bands random field generator. *Water Resour. Res.* **25** (10), 2227–2243.

Zechman, E. M. 2005 *Improving Predictability of Simulation Models Using Evolutionary Comutation-based Methods for Model Error Correction*. PhD dissertation, North Carolina State University, Raleigh, NC.

Zechman, E. M. & Ranjithan, R. 2004 An evolutionary algorithm to generate alternatives (EAGA) for engineering optimization problems. *Eng. Optimiz.* **36** (5), 539–553.

Zechman, E. M. & Ranjithan, R. S. 2007 Generating alternatives using evolutionary algorithms for water resources and environmental management problems. *J. Wat. Resour. Plan. Manage. ASCE* **133** (2), 156–165.

First received 6 December 2007; accepted in revised form 28 August 2008